A Compact Multi-Band Metamaterial-Inspired Antenna Incorporating Shorting Pins

Ali Jafargholi[1], and Amir Jafargholi[1, 2]
[1] Electromagnetic and Antenna Lab., Amirkabir University of Technology, 424 Hafez Ave., P.O. Box 15875-4413, Tehran, Iran
[2] Department of Energy Engineering and Physics, Amirkabir University of Technology, P.O. Box: 15875-4413, Tehran, Iran
E-mail: jafargholi@ieee.org (Corresponding author)

ABSTRACT:
The capability of complementary capacitively-loaded-loop (CCLL) inspired metamaterial (MTM) to miniaturize printed patch antenna is examined. The cell etched at the antenna ground plane. The antenna is comprised of three main sections: CCLL cell, shorting pins, and a patch with the overall dimensions of 50×25 mm^2. It is shown that the MTM structure exhibits a magneto-dielectric behavior at the lower frequencies. With the aid of the effective material, a miniaturized printed patch antenna operates at 650 MHz has been achieved. In some frequency bands, the MTM structure efficiently provides an artificial magnetic conductor (AMC). This later feature helps to achieve efficient multi-band operation and the antenna can cover the required frequency band of the most commercial wireless communication systems, such as LTE 2500/2600 (2480 to 2730 MHz), radiolocation service (2890 to 3110 MHz) and LTE 3500/3700, WLAN 3600 (3640 to 3880 MHz). In order to validate the simulation results, a prototype of the antenna is fabricated and tested. Good agreement between the simulation and measurement results is obtained.

KEYWORDS: Miniaturized Antenna, Multi-band Antenna, Metamaterials

1. INTRODUCTION

The increasing demands on compact multifunctional devices have necessitated the development of multi-frequency printed antennas [1]. In recent years, many works have been devoted to miniaturizing different types of antennas. The typical difficulties encountered in designing compact antennas include narrow bandwidth and low radiation efficiency. Introducing metamaterials (MTMs) opened very interesting possibilities for the improvement of antenna and microwave components. Researchers have demonstrated metamaterial to achieve high gain [2], [3], low-cross polarization [4], broad bandwidth [5] and miniaturized antennas, including antennas on reactive impedance substrate [6], high impedance wire [7], incorporating electromagnetic band-gap (EBG) structures [8], and composite right/left-handed (CRLH) structures [9]-[12]. Artificial magnetic conductors (AMCs) based on capacitively loaded loop (CLL) first introduced by Ziolkowski in [13], have found various applications in antenna engineering [14]-[17]. In [7] using high impedance wire (HIW) incorporating CLL-MTM structure a new miniaturized microstrip antenna is presented. Besides this AMC behavior, in this paper, it is shown that a CLL-MTM has different effective behavior when etched at the microstrip antenna ground plane. It is shown that this MTM-cell provides a magneto-dielectric response with high permittivity and permeability. Thanks to CLL behavior, this paper presents a compact multiband printed patch antenna. It is shown that loading antenna by a single-cell complementary CLL (CCLL) structure, a miniaturized multi-band low-profile antenna has been achieved. Moreover, the metamaterial-inspired structure helps the antenna to have high radiation efficiency at the higher frequency bands. Although the MTM was known as a periodic structure, applying an element such as a unit-cell of MTM in antenna structure as a metamaterial-inspired antenna has been studied and unusual properties of the MTM have been achieved [18], [19].

It has been shown in [20] that by inserting shorting pins at a proper position between ground and patch, such parameters like gain, directivity, and efficiency of an antenna can be improved. Here, by adding the shorting pins, the radiating field strength is drastically enhanced especially at the radiating edge of the patch. These pins reverse the surface current. Reversing the surface current at the edge causes to improve the antenna radiation. The proposed CCLL–loaded patch antenna has a dimension of approximately $0.11\lambda_L \times 0.055\lambda_L \times 0.001\lambda_L$ (f_L = 650 MHz and λ_L is the free space wavelength corresponding to the lower frequency) while achieving a gain and an efficiency of -16~5.5 dB and 5~75%, respectively. Although the antenna gain at the low-frequency band is not adequate for communication applications, its compact size could

تاریخ دریافت: ۱۳۹۸/۰۲/۱۹ تاریخ پذیرش: ۱۳۹۸/۱۲/۰۱

attract engineers who want to manufacture compact receivers. The suggested structure is fabricated and the simulation results are confirmed by measurements.

2. ANTENNA CONFIGURATION

The antenna is comprised of three main sections: CCLL cell, two shorting pins, and a patch. As described in the previous section, a CCLL structure have been used to achieve a miniaturized patch antenna that operates at a frequency that is much lower than that of a resonant frequency of a conventional unloaded patch antenna. This resonant frequency adjusted by tuning the MTM cell size. To achieve a more compact structure, the cell is fabricated by etching the antenna ground plane. In this section, the constituent parameters of the cell are investigated.

2.1. Metamaterial Cell Design

It is well known that the operating frequency of a microstrip antenna decreases by increasing the patch size. Moreover, the bandwidth and the resonance frequency of a patch are related to the substrate constitutive parameters by

$$f_r \propto \frac{1}{\sqrt{\varepsilon\mu}} \tag{1}$$

Eq. 1, shows that to having a miniaturized antenna, the antenna substrate permittivity (ε) and permeability (μ) should be high. In this section, we try to find an MTM cell with such a desired frequency response.

Assuming a periodic structure, the constituent parameters of the CCLL cell are investigated. Fig. 1 shows the schematic of the unit-cell. To understand how to choose the incident electric/magnetic field vectors we have to study the electromagnetic fields' directions of a conventional patch antenna. The electric field of a patch is parallel to the antenna surface (in the *y*-direction) while its magnetic field has a circulation behavior (in the *x*-direction). In order to retrieve the constituent parameters of the proposed metamaterial, the periodic response is extracted by applying perfect electric conductor (PEC) boundaries in the *xz*-plane and a pair of perfect magnetic conductor (PMC) boundaries in the *yz*-plane. Also, a pair of wave-ports is assigned on the *xy*-plane. The resultant scattering parameters obtained from CST microwave studio are exerted to Chen's algorithm [21]. The normalized impedance (z) and refractive index (n) of the model can be calculated as follows:

$$z = \pm\sqrt{\frac{(1+S_{11})^2 - {S_{21}}^2}{(1-S_{11})^2 - {S_{21}}^2}}, real(z) \geq 0$$
$$n = \frac{1}{k_0 d}\{[\ln(e^{\acute{\imath}nk_0d})] + 2m\pi] - i[\ln(e^{\acute{\imath}nk_0d})]\} \tag{2}$$

where d is the MTM cell thickness and k_0 is the free space wave number and

$$Im(n) \geq 0, e^{ink_0d} = \frac{S_{21}}{1 - S_{11}\frac{z-1}{z+1}} \tag{3}$$

The ambiguity of the value of m in (2) is resolved using Kramers-Kronig (KK) relating the real and imaginary parts of the index of refraction

$$Re\big(n(\omega)\big) = 1 + \frac{2}{\pi}P.V.\left[\int_0^\infty \frac{\acute{\omega}\, Im\big(n(\acute{\omega})\big)}{\acute{\omega}^2 - \omega^2} d\acute{\omega}\right] \tag{4}$$

where *P.V.* denotes the principal value of the integral. The effective permittivity (ε) and permeability (μ) of the medium can be expressed as $\varepsilon=n/z$, $\mu=nz$. Using an FR4 substrate with a dielectric constant of ε_r=4.4, and a substrate thickness of 0.762 mm, Fig. 1(b) shows the retrieved effective parameters of the cell. The design parameters of the cell are labeled in Fig. 2. The MTM unit-cell exhibits a magneto-dielectric behavior in three frequency ranges including up to 0.6 GHz, between 0.9 and 2.4 GHz, and through 2.5 to 3.0 GHz. According to this figure, the retrieved effective $\varepsilon_r \times \mu_r$ of the medium at these regions are high which is preferred for antenna miniaturization. Moreover, the MTM unit-cell shows AMC characteristics at f = 0.8, 2.7 and 3.75 GHz.

2.2. Antenna Design

A microstrip patch antenna has been considered. The schematic of the proposed pin loaded patch antenna and the fabricated prototype are shown in Fig. 2. The antenna is represented as a perspective view, from the front and the back. The antenna is printed on a 25.1 × 50 mm^2 single layer FR4 substrate with a dielectric constant of 4.4 and a thickness of 0.762 mm and the patch size is about 15 × 29.5 mm^2. The CCLL cell is etched at the antenna ground plane. The shorting pin is located near the antenna edge to demonstrate miniaturization. The pin is located at a distance t away from the edge of the patch. An additional pin with a distance of W_1 away from the edge is implemented between the patch and the antenna ground plane. This pin inverses the electric field direction and it causes increasing the field strength at the radiating edge significantly. Both pins have a radius of r = 0.5 mm. To feed the antenna, a microstrip line connected to an SMA connector is used. The width of the feed line is W_f while its length is L_f. The antenna parameters are labeled in the figure caption. This prototype is fabricated and tested (See Fig. 2(b)).

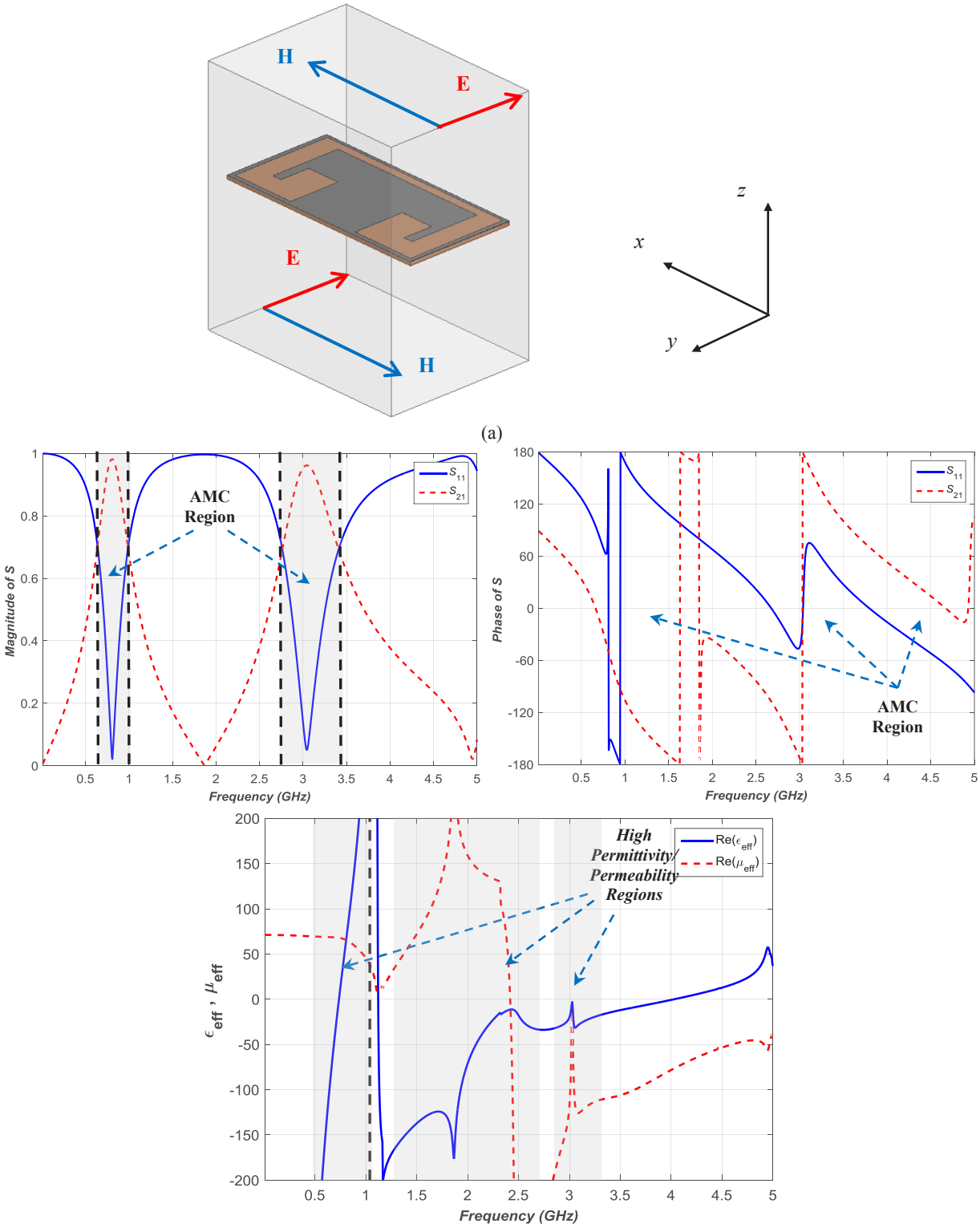

Fig. 1. The CCLL cell, (a) schematic of the cell, the cell dimensions are summarized in Fig. 2, and (b) the magnitude and phase of the S-parameters and the constitutive parameters

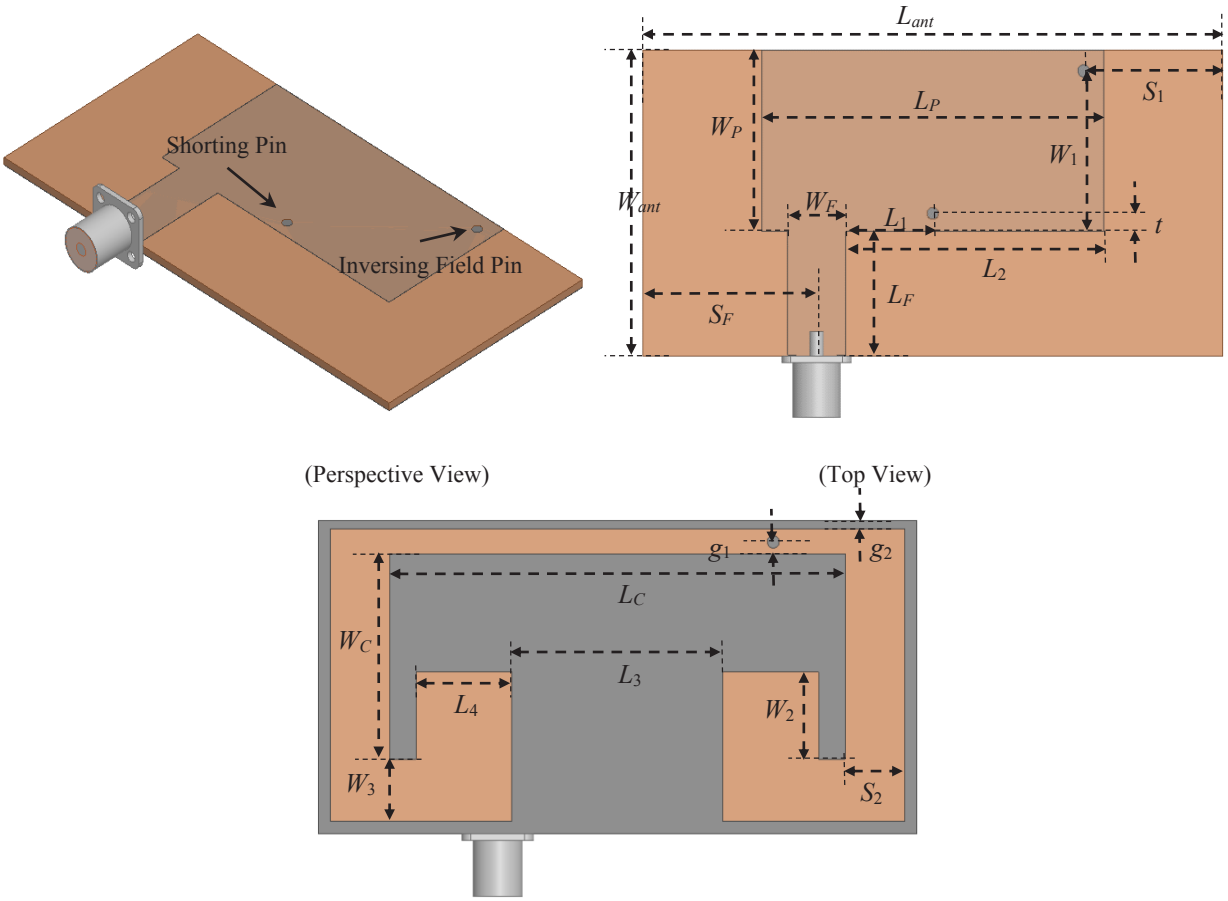

Fig. 2. Geometry of CCLL–loaded patch antenna: L_{ant}=50 mm, W_{ant}=25.1 mm, L_P=29.5 mm, W_P=14.89 mm, L_F=10.15 mm, W_F=5 mm, S_F=12.5 mm, L_C=38 mm, W_C=16.5 mm, W_1=13.2 mm, W_2=7 mm, W_3=5 mm, L_1=7.5 mm, L_2=22.25 mm, L_3=17.6 mm, L_4=8 mm, t=1.5 mm, S_1=12 mm, S_2=5 mm, g_1=0.95 mm, and g_2=0.65 mm, (a) Schematic view, and (b) Antenna prototype

3. SIMULATION AND TEST RESULTS

Fig. 3 shows the antenna impedance components and the simulated and measured s-parameters of the antenna with and without CCLL-load. Fig. 3(a) shows the measured reflection coefficient of the antenna as compared with the simulation results with and without the CCLL-loads. Good agreement between simulation and measurement results is obtained. The antenna shows a low- frequency band that could be tuned by adjusting the CCLL-cell size. Here, it is adjusted to cover 650 MHz with the impedance bandwidth of 3% (20 MHz) from 643 to 663 MHz. The antenna also

operates at the frequency bands that expanded from 2480 to 2730 MHz (LTE 2500/2600), 2890 to 3110 MHz and 3640 to 3880 MHz (LTE 3500/3700, WLAN 3600). The antenna bandwidth is 9.6% (250 MHz), 13.5% (420 MHz), and 6.4% (240 MHz) for these bands, respectively. The antenna designed to operate in portable handheld applications, thus the frequency bands extracted using $|S_{11}|<-6\ dB$.

The resonant frequency of a simple patch antenna printed on the same dielectric substrate with a patch length of 50 mm is 2.1 GHz (See Fig. 2). Comparing this resonance with that obtained in the proposed antenna, 650 MHz, more than 69% size reduction is achieved. The antenna has a dimension of approximately $0.11\lambda_L \times 0.055\lambda_L \times 0.001\lambda_L$ (f_L = 650 MHz and λ_L is the free space wavelength corresponding to the lower frequency). The real component of the input impedance is illustrated in Fig. 3(b). According to this figure, adding both shorting pins and using CCLL cell causes to obtain a more compact antenna.

In Fig. 3(c), the behavior of the loaded antenna as a function of CCLL cell size is investigated. Due to the resonating nature of the CCLL, it is expected that the S-parameter of the antenna affected considerably. The numerical simulations show that the antenna return loss significantly affected by the metamaterial cell size. In this figure, we define a scale factor that compares the antenna return loss for proposed CCLL cell size with the smaller cells.

Parameter L_{DGS} defines the meander-line length and the defect on the ground plane. This parameter may be adjusted to enhance antenna bandwidth. Fig. 3 shows simulated reflection coefficient of the proposed antenna for different values of L_{DGS}. According to this figure, parameter L_{DGS} could significantly affect the antenna impedance characteristics.

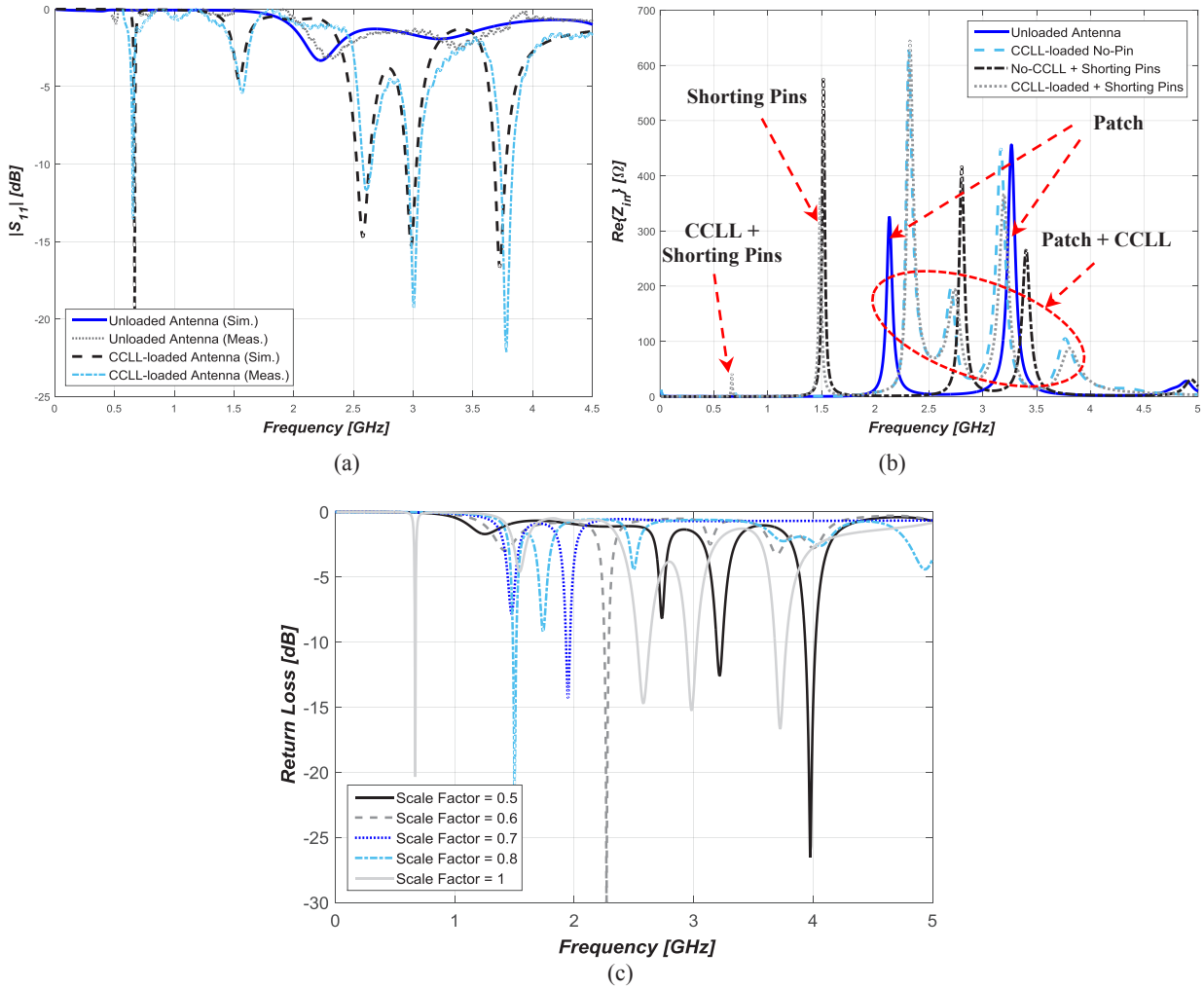

Fig. 3. Measurement and simulation results of the CCLL-loaded slot and unloaded antennas, (a) Reflection coefficients, and (b) Real component of the input impedance, and (c) simulated antenna return loss as a function of CCLL cell size

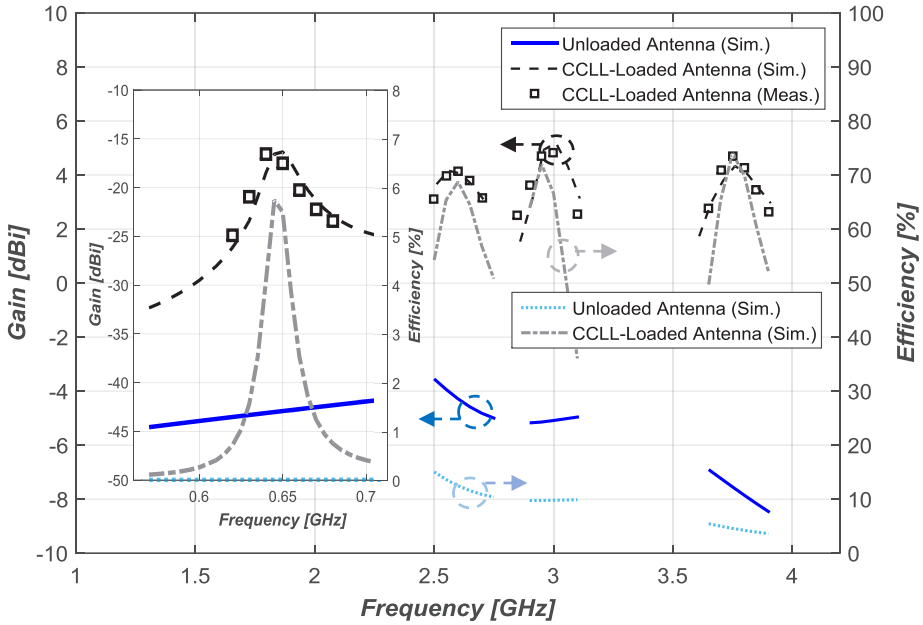

Fig. 4. Measured peak gain and simulated radiation efficiency of the loaded and unloaded antennas versus frequency

The measured gain and the simulated radiation efficiency of the antenna with (solid line) and without (dashed-line) CCLL-loads are compared in Fig. 4. It is clear that the radiation efficiency of the antenna at the lower band frequencies is higher than 5% along with a gain of >-16dBi. These parameters at the higher bands are in the range of 50~75% and 0~2.7dBi, However, respectively. As shown in Fig. 4, the measured gain is almost close to those obtained by the simulation. According to this figure, the antenna gain and efficiency at the low-frequency band are not preferred for communication applications. However, in contrary to the unloaded patch, the CCLL-loaded antenna has a considerable performance. At the lower frequencies, the unloaded antenna could not be matched and the antenna gain and efficiency is drastically lower than those obtained by the loaded antenna. Talking about the radiation performance, a fair comparison might be done with an unloaded patch antenna whose resonating at the same frequency. Since, the main objective of this paper is to investigate the effect of CCLL on a simple patch antenna, in this paper we compared an unloaded antenna with the loaded antenna has the same overall dimensions.

Fig. 5 shows the distribution of the tangential component of the electric field at f = 650 MHz. According to this figure, the radiated field strength is substantially low at the unloaded antenna. Loading the original patch antenna by means of CCLL the magnitude of the electric field increased markedly. As described before (see Fig. 1(b)) the CCLL cell behaves like an AMC material. The AMC-MTM helps to modify electric field directions. Adding the shorting pins, the radiating field strength is drastically enhanced especially at the radiating edge of the patch. These pins reverse the surface current. Reversing the surface current at the edge causes to improve the antenna radiation

The normalized measured far-field radiation of the antenna is depicted in Fig. 6 at f = 650 MHz, 2.6, 3, and 3.7 GHz. It is clear that the antenna has omnidirectional radiation at f=650 MHz. At this frequency, the antenna electrical size is small, $0.11\lambda_L$, and the antenna *exhibits* dipolar *radiation*. At the higher frequencies, since the CCLL-cell is fabricated by etching the antenna ground plane the radiation pattern has a bi-directional behavior. This feature is beneficial for handheld/portable devices since the position of them are non-predictable in practical applications [22]. Some slight asymmetry is attributed due to the offset in the ground plane afforded by the physical SMA connector and shorting pins location. The cross-polarization discrimination of >10 dB is obtained at both E- and H-planes.

Table 1 shows the overall performance of the CCLL-MTM loaded patch antennas in comparison with the recently reported antennas [23]-[25]. Deficiencies of the reference antennas are highlighted in the table. Both the maximum radiation efficiencies, η, and maximum gain measured in the two operating bands of the proposed antenna are comparable with all the references. The first paper addressed in the table introduces a simple compact antenna comprised of a U-shaped slot antenna with a coupling feed for 4G handset applications. A compact multi-band antenna consists of a C-shaped and U-shaped monopole coupled to an F-shaped strip connected with the ground in the bottom layer is introduced in [24]. In [25], a multi-broadband planar antenna is proposed which consists of a folded monopole, a C-shaped monopole, and a trapezoidal monopole with an inverted-F monopole. These two designs are also suffering by the large size of the ground plane.

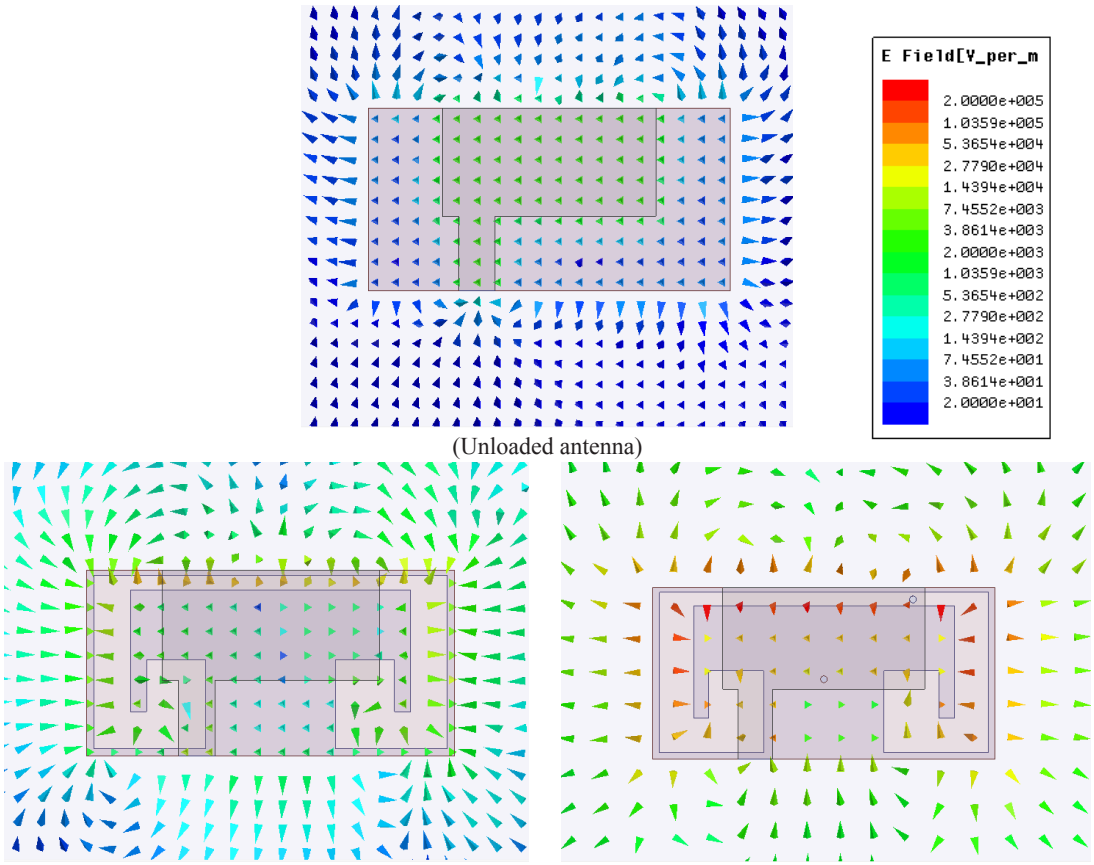

(Unloaded antenna)

(CCLL-loaded antenna) (CCLL-loaded antenna incorporating shorting pins)

Fig. 5. Simulation results of the electric field distribution at *f*=650 MHz

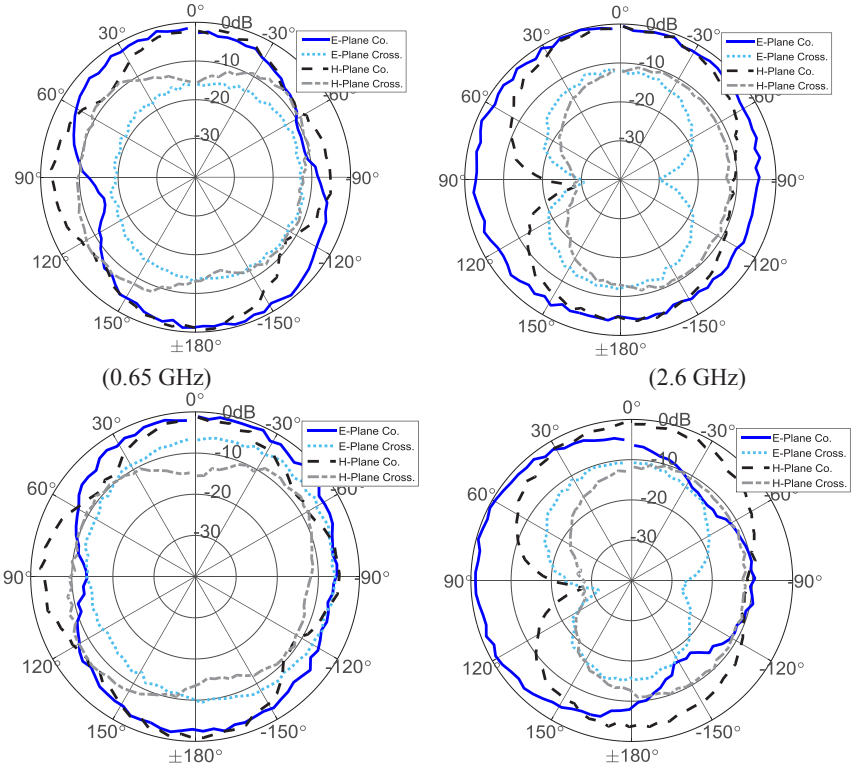

(0.65 GHz) (2.6 GHz)

(3 GHz) (3.7 GHz)

Fig. 6. Measured Normalized radiation patterns of the CCLL-loaded antenna

Table 1. Summary of antenna performances for the proposed and reference antennas

Antennas	Max Gain (dBi)	Max η (%)	Number of Band	Dimension (mm)	Operating Frequency Bands (MHz)
Ref [23]	0.8/0.6~2.1	50~85	Dual	120×65×0.6	690–750/1700–4200
Ref [24]	2.8/4.3/4.4/5.6	50~87	Multi	15×68×0.8 +121×68 Ground	698–1046*/1618–2703*/3018–4377*/4697–6000*
Ref [25]	1/2/5	65~85	Multi	15×60×0.5 +100×60 Ground	790–1061*/1650–2775*/3132–6382*
This Work	-16/4.1/5/5.5	5.5/68~75	Multi	25×50×0.762	643–663*/2480–2730/2890–3110/3640–3880

* The bandwidth measured by using $|S_{11}|<-6$ *dB*

4. CONCLUSION

A compact, multi-band and low-profile patch antenna for handheld/portable applications has been presented. It is shown that utilizing a CCLL helps to obtain prevalent LTE/WLAN frequency bands. Adding two shorting pins causes to reverse the antenna surface current which consequently leads to improve radiating performance. The MTM cell etched on the antenna ground plane. The antenna has a low-profile configuration and fed by a simple microstrip line. The antenna overall dimension is $0.11\lambda_L \times 0.055\lambda_L \times 0.001\lambda_L$ while it achieves gain and efficiency of -16~5.5 dB and 5~75%, respectively.

REFERENCES

[1] A. Jafargholi, M. Kamyab, M. Veysi, and M. Nikfal Azar, "Microstrip gap proximity fed-patch antennas, analysis, and design," *AEU – Int. J. Electronics and Comm.*, vol. 66, no. 2, pp. 115-121, 2012.

[2] M. Sinha, V. Killamsetty, and B. Mukherjee, "Near Field Analysis of RDRA Loaded with Split Ring Resonators Superstrate," *Microwave Optical Technology Lett.*, Wiley, vol. 60, no. 2, pp. 472-478, 2018

[3] M. Veysi, and A. Jafargholi, "Directivity and Bandwidth Enhancement of Proximity-Coupled Microstrip Antenna Using Metamaterial Cover" *Applied Computational Electromagnetics Society Journal*, vol. 27, no. 11, 2012.

[4] A. Jafargholi and M. H. Mazaheri, "Broadband microstrip antenna using epsilon near zero metamaterials," *IET Microwave Antenna Propag*, vol. 9, no. 14, pp. 1612-1617, 2015.

[5] B. Mukherjee, P. Patel, and J. Mukherjee, "A Novel hemispherical Dielectric Resonator Antenna with Complimentary Split Rings shaped slots and resonator for wideband and low cross-polar applications," *IEEE Antenna and Propagation Magazine*, vol. 57, no. 1, pp. 120-128, 2015

[6] H. Mosallaei, K. Sarabandi, "Antenna miniaturization and bandwidth enhancement using a reactive impedance substrate," *IEEE Trans. Antennas. Propag*., Vol. 52, pp. 2403–2414, 2004.

[7] A. Jafargholi, and M. Mohammadkhani, "Miniaturized Microstrip Antenna Using High Impedance Wires Incorporating AMC MTMs," *Int. J. Electronics Lett*., vol. 4, no. 4, pp. 489–496, 2016.

[8] Y. Rahmat-Samii and F. Yang, *Electromagnetic Band Gap Structures in Antenna Engineering. Cambridge*, U.K.: Cambridge Univ. Press, 2009.

[9] M. Rafaei Booket; M. Veysi; Z. Atlasbaf; A. Jafargholi, "Ungrounded Composite Right/Left Handed Metamaterials: Design, Synthesis, and Applications," *IET Microwave Antenna Propag*., Vol. 6, No. 11, pp. 1259-1268, 2012.

[10] N. Amani, A. Jafargholi, "Zeroth-Order and TM_{10} Modes in One-Unit Cell CRLH Mushroom Resonator", *IEEE Antennas Wirel. Propag. Lett*., Vol.14, 1396–1399, 2015.

[11] N. Amani, A. Jafargholi, M. Kamyab, and A. Vaziri, "Asymmetrical wideband zeroth-order resonant antenna," *Electronics Lett*., vol. 50, no. 2, pp. 59-60, 2014.

[12] N. Amani, M. Kamyab, A. Jafargholi, A. Hosseinbeig, and J. S. Meiguni, "Compact tri-band metamaterial-inspired antenna based on CRLH resonant structures," *Electronics Lett*., vol. 50, no. 12, pp. 847-848, 2014.

[13] A. Erentok, P. Luljak, and R. W. Ziolkowski, "Characterization of a volumetric metamaterial realization of an artificial magnetic conductor for antenna applications," *IEEE Trans. Antennas Propagat.*, vol. 53, pp. 160–172, Jan. 2005.

[14] A. Jafargholi, M. Kamyab, and M. Veysi, "Artificial magnetic conductor loaded monopole antenna," *IEEE Antennas Wireless Propag. Lett*., vol. 9, pp. 211–214, 2010.

[15] A. Jafargholi, and A. Jafargholi, "Miniaturization of Printed Slot Antennas Using Artificial Magnetic Conductors," *IET Microwave Antenna Propag*., vol. 12, no. 7, 1054-1059, 2018.

[16] A. Jafargholi, M. Kamyab, M. Rafaei Booket, and M. Veysi, "A compact dual-band printed dipole antenna loaded with CLL-based metamaterials" *Int. Rev. Electrical Engineering*, vol. 5, no. 6, 2010.

[17] A. Jafargholi, A. Jafargholi and B. Ghalamkari, "Dual-Band Slim Microstrip Patch Antennas," *IEEE Trans. Antennas Propagat*., vol. 66, no. 12, pp. 6818-6825, 2018.

[18] R. W. Ziolkowski, P. Jin, and C.-C. Lin, "Metamaterial-Inspired Engineering of Antennas," *IEEE Proc*., Oct. 2011.

[19] M. Rafaei Booket, A. Jafargholi, M. Kamyab, H. Eskandari, M. Veysi, and S. M. Mousavi, "A Compact Multi-Band Printed Dipole Antenna Loaded with Single-Cell MTM," *IET Microwave Antenna Propag*., vol. 6, no. 1, pp. 17–23, 2012.

[20] A. Jafargholi, A. Jafargholi, and J. H. Choi, "Mutual Coupling Reduction in an Array of Patch Antennas

Using CLL Metamaterial Superstrate for MIMO Applications," *IEEE Trans. Antennas Propagat*., vol. 67, no. 1, pp. 179-189, 2019.

[21] Z. Szabó, G. H. Park, R. Hedge, and E. P. Li, "A Unique Extraction of Metamaterial Parameters Based on Kramers–Kronig Relationship," *IEEE Trans. Microwave Theory Tech*., vol. 58, no. 10, 2646–2653, 2010.

[22] N. Amani, A. Jafargholi, "Internal Uni-Planar Antenna for LTE/WWAN/GPS/GLONASS Applications in Tablet/Laptop Computers", *IEEE Antennas Wirel. Propag. Lett*., vol. 14, pp. 1654–1657, 2015.

[23] C. Hsu and S. Chung, "Compact Antenna With U-Shaped Open-End Slot Structure for Multi-Band Handset Applications," *IEEE Trans. Antennas Propag*., vol. 62, no. 2, pp. 929-932, Feb. 2014.

[24] X. Wang, Y. Wu, W. Wang, and A. A. Kishk, "A Simple Multi-Broadband Planar Antenna for LTE/GSM/UMTS and WLAN/WiMAX Mobile Handset Applications," *IEEE Access*, vol. 6, pp. 74453-74461, 2018.

[25] H. Liu, R. Li, Y. Pan, X. Quan, L. Yang, and L. Zheng, "A Multi-Broadband Planar Antenna for GSM/UMTS/LTE and WLAN/WiMAX Handsets," *IEEE Trans. Antennas Propag*., vol. 62, no. 5, pp. 2856-2860, May 2014.